

# Numerical and Parametric Studies on Flexural Behavior of ECC Beams by Considering the Effect of Fly-Ash and Micro-PVA Fiber

Kh. M. Hind<sup>\*,a</sup>, M. Özakça<sup>b</sup> and T. Ekmekyapar<sup>c</sup>

Department of Civil Engineering, University of Gaziantep, 27310 Gaziantep, Turkey

<sup>a,\*</sup>hindmahmood18@gmail.com, <sup>b</sup>ozakca@gantep.edu.tr, <sup>c</sup>ekmekyapar@gantep.edu.tr

**Abstract** - Engineered cementitious composite (ECC) refers to the group of cementitious mixtures possessing the strain-hardening and crack control abilities. The mechanical performance of ECC beams will be investigated with respect to the effect of aggregate size and amount, by using nonlinear finite element method and nonlinear parametric study. The comparative analysis showed that an increase in the total size and quantity, there was observed no particular change in flexural strength, while the ductility of ECC had a negative influence. Besides, the ECC beams were observed to cause significant improvements in flexural stress, strain, and midspan deflection when measured against the reference beam (microsilica MSC), i.e. the average improvement percentages were 70.33%, 1116.67%, and 1256.78%, respectively. These results are quite similar to that of the experimental results, which provides that the finite element model is in accordance with the desirable flexural behaviour of the ECC beams.

**Keywords:** engineered cementitious composite (ECC), flexural behaviour, ductility, finite element modelling, parametric study.

## 1.0 INTRODUCTION

Concrete is a quasi-brittle material in which upon reaching the particular tensile strength limit, crack width increases with time. In most of the structures the crack width control abilities are below satisfaction, even when having steel reinforcements. Cracking tends to decrease the durability of structures as harmful chemical substances can easily attack the concrete surfaces. For this reason various preventive measures are employed to reduce the quasi-brittle properties of concrete [1-12]. Recently, engineered cementitious composites (ECCs) have been proposed as a new class of concrete materials which have considerably greater level of ductility. ECC is a unique kind of cementitious composite having high ductility and damage tolerance properties under intense mechanical loadings, including tensile and shear loadings [13-19]. The material is optimized as per the principles of micromechanics [13, 20-24] which increases the tensile strain capacity of material up to 3-5% where operating uniaxial tensile loading making it achievable through only 2% polyvinyl alcohol (PVA) or polyethylene fibre (PE) quantity by volume [13, 25-27]. The strain-hardening property of ECC tends to enable significant development of multiple micro-cracks, i.e. the crack width limit remains within the range of 50 to 80  $\mu\text{m}$ , even under extreme loads.

A micromechanics-based material design theory is utilized to enhance the strength and energy ratios of the mixture proportions of ECC to acquire high composite ductility [13, 14, 28]. The crack control properties of ECCs with respect to controlling the width of occurring cracks

depend upon the type, size, and amount of fibre, matrix ingredients and interface properties of the material. The manufacture of ECCs is done by using particular quantities of high-quality mixtures, which when accompanied by the bristly material in the paste, helps to enhance the matrix (ECC without fibre) toughness. As a result, the material attains the crack control characteristics i.e. delayed crack initiation and prevention of steady-state flat-crack propagation which might cause to reduce the tensile ductility of ECC [27, 29, 30]. Furthermore, if the mixtures include large sized particles as compared to the standard size of fibre spacing, it may lead to cause balling of fibres which may result in disturbing the uniformity of fibre dispersion [31, 32]. This proposes that ECC with fine aggregate must have a standard aggregate/binder ratio (A/B) of 0.36 and a maximum grain size of 250  $\mu\text{m}$  [27, 33].

Owing to various ecological and economical reasons, industrial by-products are now used as supplementary materials in the manufacture of different classes of concrete mixtures. Fly ash (FA) is the most widely used and extensively available mineral admixture. However, in the past few years, FA has been used as a substitution of cement with regard to its application in ECC [34-36]. Higher concentration of cement is obtained when coarse aggregate is absent in ECC. Furthermore, partial replacement with FA helps to reduce ecological loadings. As mentioned previously, using larger quantities of mineral admixtures, particularly FA, helps decreasing the strength of matrix while enhancing that of ECC with respect to tensile ductility [36-38]. Moreover, anhydrite mineral admixtures having small particle size and even spherical shape are utilized as filler particles, providing higher density of the fibre/matrix interface transition zone resulting to produce high frictional bonding [36, 39-41]. This enhances long-term stability of the structure by significantly decreasing the steady-state crack width.

Employing high-volume mineral admixture in the manufacture of ECC can lead to cause an increase in the amount and size of aggregates leading to increase the matrix strength of the material. In a research conducted by Sahmaran et al. [42, 43], the mechanical properties of high-volume FA-ECC are studied with respect to the effect of aggregate size. The obtained results showed that the aggregate size of up to 2.38 mm, did not affect the ductility of ECC as it had no effect on the uniform fibre dispersion. The quantity of aggregates is subjected to increase, along with the identification of a substituent type of mineral admixture for FA. Nevertheless, the flexural behaviour of the ECC beams has not been brought to considerable research with regard to its numerical aspects. Besides, the potential influence of aggregate amount and size upon the tensile behaviour and dimensional constancy of ECC has also not studied in terms of both unrestricted as well as restrained contraction of material. It is aimed to bring this area of knowledge under research.

This research intends to study the effect of an increase in the amount and size of aggregate material, on the flexural properties of ECC beams by using 3D nonlinear finite element simulation model through ANSYS software. The developed FE models were validated by comparing the numerical results with experimental data available in literature [44]. To study the effect of various factors upon the flexural stress and flexural deflection, a nonlinear parametric study was made. As per the results obtained through this study, a model has been put forward which accounts the factors having a significant influence upon the flexural stress and flexural deflection of ECC beams. The model entails the ECC aggregate content ( $AC$ ), ECC compressive strength ( $f_{ECC}$ ), and maximum aggregate size ( $D_{max}$ ). Moreover, the experimental results obtained from the studying the 57 ECC beams as mentioned in the literature [42, 43] are used to test the validity of the newly presented model.

## 2.0 EXPERIMENTAL STUDY

In order to study the flexural behaviour of ECC beams, six ECC beams with dimensions of (360×50×75) mm, have been modelled and compared with Microsilica concrete beam (MSC) model, as shown in Fig. 1. Microsilica is an excellent admixture for concrete as it leads to better engineering properties. It reduces thermal cracking, improves durability, and increases strength. However, the beams were designed to be simply supported over a clear span of 304 mm and subjected to four-point loading. The basic mixture ingredients in ECC were: two different fine aggregate sizes (400 and 1000)  $\mu\text{m}$ , three aggregate contents (0.36, 0.45, and 0.55 A/B), Fly ash (FA) mineral admixture type, (1.2 FA/C ratio) mineral admixture replacement rate and a constant water-binder ratio ( $w/b$ ) of 0.27 are considered. Details of this factorial design and designation of mixtures are presented in Table 1. PVA fiber 8 mm in length and 39 $\mu\text{m}$  in diameter extensively used in this study. To account for material inhomogeneity, a PVA fiber content of 2% by volume has been typically used in the mixture design. Table 2 illustrate the mechanic and geometric properties of PVA fibers. All the used data in this study based on confirmed experimental results, which have been achieved by [44].

### 3.0 NUMERICAL MODELLING OF ECC BEAMS

ANSYS program was employed to choose the best element/model in order to suit the experimental investigation. The program is able to deal with the particular numerical models designed to account for the nonlinear course of actions of concrete and ECC beams operating under invariable loadings. The ECC beams and Microsilica concrete (MSC) were modelled by using SOLID 65 elements. These elements entails eight nodes with three levels of freedom at each node and transformations in the nodal x-, y- and z-directions. SOLID 65 elements hold the properties of plastic deformation, three dimensional cracking and crushing. ANSYS uses linear isotropic and multi-linear isotropic material attributes for modelling concrete, along with supplementary concrete material properties, for replicating actual concrete behaviour [45].

According to the William and Warnke model [46], the concrete element in tension will crack and lose stiffness upon reaching its tensile strength. Therefore, the behavior of the concrete element in tension was modeled as linear elastic up to the concrete tensile strength. The state of cracked surface is indicated through the shear transfer coefficient  $\beta_t$ , whose value ranges from 0.0 to 1.0, where 0.0 symbolizes a smooth crack while 1.0 represents a coarse crack [47, 48]. In this study, the value of shear transfer coefficient of an open crack,  $\beta_t$  is 0.2 [49] while the value of shear transfer coefficient of a closed crack,  $\beta_c$  is 0.8 [50]. For ECC beams,  $\beta_t=0.05$  and  $\beta_c=0.45$ , were adopted [51].

The equation  $E_c = 4700\sqrt{f'_c}$ , used to calculate the modulus of elasticity of the MSC while the tensile strength computed from the equation  $f_r = 0.62\sqrt{f'_c}$ . The Poisson's ratio value used is 0.2. Furthermore, the following equations for the multi-linear isotropic stress–strain curve were used to obtain the compressive uniaxial stress–strain values for the MSC model [49, 50]:

$$E_c = f_{el} / \varepsilon_{el}, \quad \varepsilon_o = \frac{2f'_c}{E_c} \quad \text{and} \quad f = \frac{E_c \varepsilon}{1 + (\varepsilon / \varepsilon_o)^2} \quad (1)$$

In this equation,

- $f_{el}$  represents the stress at the elastic strain ( $\varepsilon_{el}$ ) in the elastic range ( $f_{el} = 0.30f'_c$ ),
- $\varepsilon_o$  represents the strain at the ultimate compressive strength,

- $\sqrt{f'_c}$  represents the compressive strength of the concrete obtained from testing cylinders,
- $f$  is the stress at any strain  $\varepsilon$

For ECC beams, the typical stress-strain curves acquired from uniaxial tension and compression experiments are represented through dotted lines as shown in Fig. 2 [38, 52-54]. The following equations were used to obtain the tensile stress-strain relationship of ECC [55]:

$$\sigma_t = \frac{\sigma_{tc}}{\varepsilon_{tc}} \varepsilon \quad 0 \leq \varepsilon < \varepsilon_{tc} \quad (2)$$

$$\sigma_t = \sigma_{tc} + (\sigma_{tu} - \sigma_{tc}) \left( \frac{\varepsilon - \varepsilon_{tc}}{\varepsilon_{tu} - \varepsilon_{tc}} \right) \quad \varepsilon_{tc} \leq \varepsilon < \varepsilon_{tu} \quad (3)$$

Where:

- $\sigma_{tc}$  represents the first cracking strength in tension,
- $\varepsilon_{tc}$  represents the strain at first cracking,
- $\sigma_{tu}$  represents the ultimate tensile strength,
- $\varepsilon_{tu}$  represents the tensile strain at  $\sigma_{tu}$

The compressive stress-strain relationship of ECC can be expressed as [55]:

$$\sigma_c = 2 \frac{\sigma_{c0}}{\varepsilon_{c0}} \varepsilon \quad 0 \leq \varepsilon < \frac{1}{3} \varepsilon_{c0} \quad (4)$$

$$\sigma_c = \frac{2}{3} \sigma_{c0} + \frac{\sigma_{c0}}{2\varepsilon_{c0}} \left( \varepsilon - \frac{\varepsilon_{c0}}{3} \right) \quad \frac{1}{3} \varepsilon_{c0} \leq \varepsilon < \varepsilon_{c0} \quad (5)$$

$$\sigma_c = \sigma_{c0} + (\sigma_{cu} - \sigma_{c0}) \left( \frac{\varepsilon - \varepsilon_{c0}}{\varepsilon_{cu} - \varepsilon_{c0}} \right) \quad \varepsilon_{c0} \leq \varepsilon < \varepsilon_{cu} \quad (6)$$

Where:

- $\sigma_{c0}$  represents the compressive strength,
- $\varepsilon_{c0}$  represents the strain at peak stress,
- $\sigma_{cu}$  represents the ultimate compressive stress (in the postpeak branch),
- $\varepsilon_{cu}$  represents the ultimate compressive strain

In this study,  $\sigma_{cu} = 0.5\sigma_{c0}$  and  $\varepsilon_{cu} = 1.5\varepsilon_{c0}$  were adopted. The dimensions of concrete elements were used as 1mm in length, 1mm in height and 1mm in width.

The PVA fibres were modelled by using Link 8 elements. This is a 3D spar element having two nodes and three levels openings at each node. It holds the property of plastic deformation [45]. In this study, bond between the concrete and the PVA fibres is considered as effective as that between nodes of corresponding concrete solid elements. This helps to bring the same nodes to share same material.

As per the finite element model, the fibres were considered as bilinear, isotropic, elastic and perfectly plastic material. A value of 0.42 was used for the poisson's ratio.

Solid 185 element [45] were used to model the loading and support plates. The solid element has eight nodes with three degrees of freedom at each node, translations in the nodal x, y, and z directions. The steel plates incorporated into the finite element models were assumed to be linearly elastic materials with an elastic modulus of 200 GPa and a poisson's ratio of 0.3.

## **4.0 VERIFICATION OF NUMERICAL MODELLING WITH EXPERIMENTAL RESULTS**

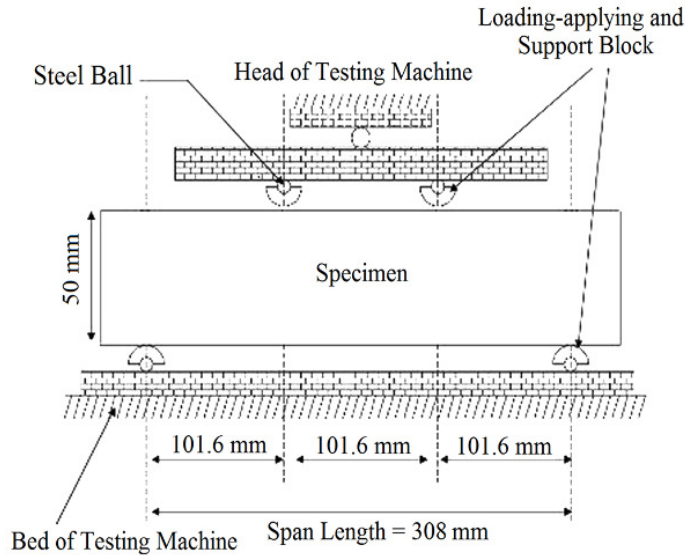
### **4.1 Load-Deflection Curves**

Fig. 3 illustrates the flexural load-midspan beam deflection curves for all the ECC beams. In the flexural load-deflection curves,

- the load at the first descend corresponded with the first cracking is termed as the first cracking load
- the maximum load is termed as the flexural load
- the corresponding deflection is termed as the flexural deflection (midspan beam deflection) capability

Fig. 3 further shows that while operating under deflecting load, ECC beams having maximum aggregate size of 1000  $\mu\text{m}$  bends similar to that of a ductile metal plate due to its property of plastic deformation. In all ECC beams, the flexural cracks prevailing at the tension surface are the first cracks to appear. Following this, the load increases along with producing multiple cracking, enhancing the inelastic deformation with an increase in stress. Microcracks produced from the first cracking point continued to extend in the midspan of the flexural beam. However, upon reaching the certain limit of fibre strength of the microcracks, bending failure in ECC took place, leading to cause a particular extent of deflection in that part when it reached its limit of flexural strength.

The average load limit for first-crack in ECC beam ranges from 920 to 1100 N with respect to the aggregate size. The aggregate size is negatively related with the crack-load i.e. an increase in the maximum aggregate size i.e. from 400 to 1000  $\mu\text{m}$ , causes a 21% decrease in the first-crack load. Besides, the extent of first-crack load of the ECC beams is not affected by variation of aggregate quantity of material. In the same way, the rigidity of the beams is also not influenced by changes in aggregate size and quantity. These results are similar to those obtained through studies conducted previously [56-58].



(a) four-point bending test

**Figure 1:** Experimental and numerical specimens

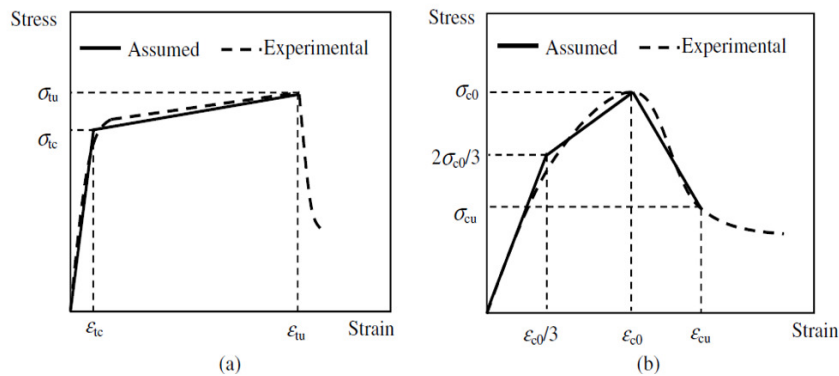


**Figure 2:** Stress-strain relationship of ECC. (a) Under uniaxial tension; (b) under uniaxial compression

**Table 1:** ECC mixture proportions containing fly ash by weight.

Specimen ID.	Cement	w/b	Aggregate/Binder		FA/C	HRWR (kg/m <sup>3</sup> )
			0-400 $\mu$ m	0-1000 $\mu$ m		
FA-1.2-0.36-400	1	0.27	0.36	-	1.2	5.1
FA-1.2-0.45-400	1	0.27	0.45	-	1.2	5.1
FA-1.2-0.55-400	1	0.27	0.55	-	1.2	5.0
FA-1.2-0.36-1000	1	0.27	-	0.36	1.2	4.9
FA-1.2-0.45-1000	1	0.27	-	0.45	1.2	5.0
FA-1.2-0.55-1000	1	0.27	-	0.55	1.2	5.0

**Table 2:** Mechanical and geometric properties of PVA fibers.

Fiber Type	Nominal Strength (MPa)	Apparent Strength (MPa)	Diameter ( $\mu$ m)	Length (mm)	Young Modulus (GPa)	Strain (%)	Specific Weight (kg/m <sup>3</sup> )
PVA	1620	1092	39	8	42.8	6.0	1300

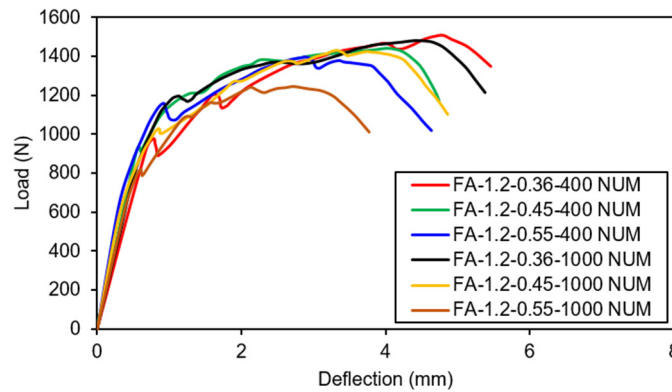


**Figure 3:** Numerical flexural load-deflection curves of ECC beams

## 4.2 Flexural Strength

The comparison between experimental and the numerical flexural strength results was shown in Fig. 4. With respect to the deflection before yield strength, the anticipated stress value of 9.43 MPa for 1000  $\mu\text{m}$  maximum aggregate size beams and 8.23 MPa for 400  $\mu\text{m}$  maximum aggregate size beams. Till the ultimate moment capacity is attained the curve is kept horizontal after the abrupt change. Moreover, the numerical results show good agreement with the experimental results.

For numerical results the average ultimate flexural strengths from 11.46 to 12.91 MPa fluctuate as seen in Fig. 4. Around 13% of ultimate flexural stress is decreased by the increase in the maximum aggregate size from 400 to 1000  $\mu\text{m}$ . In general, the flexural strength is slightly influenced by the aggregate content and maximum aggregate size as per the compressive strength results.

Table 3 demonstrates the comparison between the practical results and the simulation. The experimental results are 2% less than the average ultimate strength from the numerical simulation for 400 and 100  $\mu\text{m}$  maximum aggregate size beams. This implies that the comparative analysis is in accordance with the experimental value. Moreover, the results demonstrate that the ultimate flexural stress decreases with the increase in the aggregate content as per the maximum aggregate size which is in the accordance to the experimental value.

It is evident that the stresses of beam is increased by the increase in aggregate content and maximum aggregate size as per the contour plots of the simulation results of flexural stress shown in Fig. 5. The cracks continued to spread over the top layer of the beam after cracking, without noticeable crack width. The constant moment region was also surrounded by various minute cracks with parallel to the major one. At the same time, amid the loading process the division of various minute cracks is also starting from the centre to both supports of the beams. After initial cracking, several cracking along the specimens and minor strain hardening behaviour is quite evident. Following that, the external moment causes to distort the adhering of fibres and cementitious matrix reducing their ability to withstand the tensile stresses. In this stage the load was continues to decrease gradually once the maximum load is applied. In the end, the ECC beams failed to sustain the stress, leading to cause multiple fibre fracture, giving rise to major cracks in the midspan [40]. The experimental and numerical values for the mean percentage strength enhancement of 400  $\mu\text{m}$  maximum aggregate size ECC beams in contrast with the MSC beams were 71.73% and 73.07%, respectively. Whereas, the experimental and

the numerical values for 1000  $\mu\text{m}$  maximum aggregate size ECC beams the mean improvement percentage in-flexural stress were 66.3% and 67.6%, respectively.

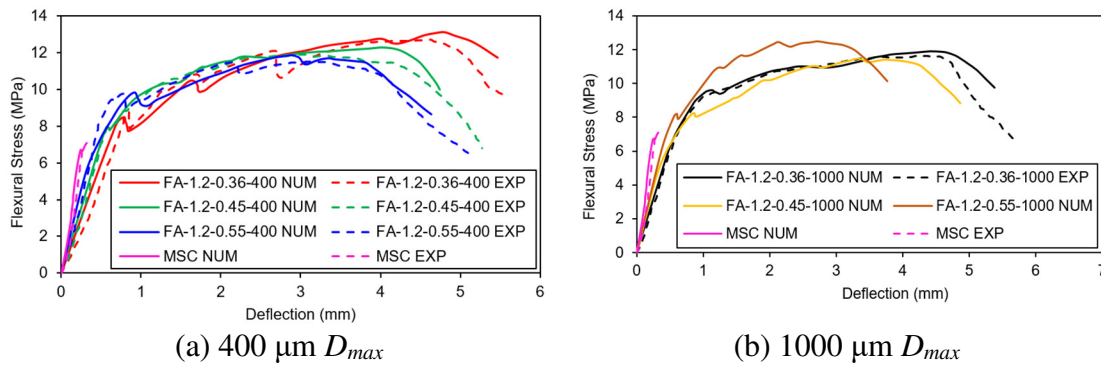


**Figure 4:** Comparison between numerical and experimental flexural stress-deflection curves of ECC and MSC beams

**Table 3:** Flexural Strength and Deflection Results of 28 Days ECC Mixtures

Mix ID.	Deflection (mm)		Flexural Strength (MPa)	
	Experimental	Numerical	Experimental	Numerical
FA1.2-0.36-400	4.83	5.30	12.73	12.91
FA1.2-0.45-400	4.23	4.40	11.92	12.07
FA1.2-0.55-400	3.97	3.89	11.41	11.69
FA1.2-0.36-1000	4.59	4.88	11.63	11.84
FA1.2-0.45-1000	4.14	4.18	11.12	11.46
FA1.2-0.55-1000	3.15	3.40	12.17	12.35

### 4.3 Flexural Strain

It has been shown from Fig. 6 that there is a decrease in maximum strain and deflection by percentage of 31.82% and 36.25%, respectively when aggregate quantity of 400  $\mu\text{m}$  maximum aggregate size of ECC beam is increased. In the same manner for 1000  $\mu\text{m}$  maximum aggregate size ECC beams the respective percentages are 42.11% and 43.53%, respectively. As provided in Fig. 7, according to the simulation results of flexural strain for ECC beams, when the aggregate size is increased from 400 to 1000  $\mu\text{m}$  there occurs a decrease in the flexural strain limit by percentage of 9%. Hence, this propose that the presence of high aggregate content and coarse aggregates in a cementitious paste may lead to increase the matrix (ECC without fibre) strength, which helps to reduce the initiation period of cracking process and averts the development of steady-state flat-cracking which may cause to decrease the tensile ductility of ECC [27, 29, 30]. Furthermore, using aggregates having a particle size larger than the average fibre spacing may cause balling of fibres, leading to provide inadequate fibre dispersion uniformity [31, 32].

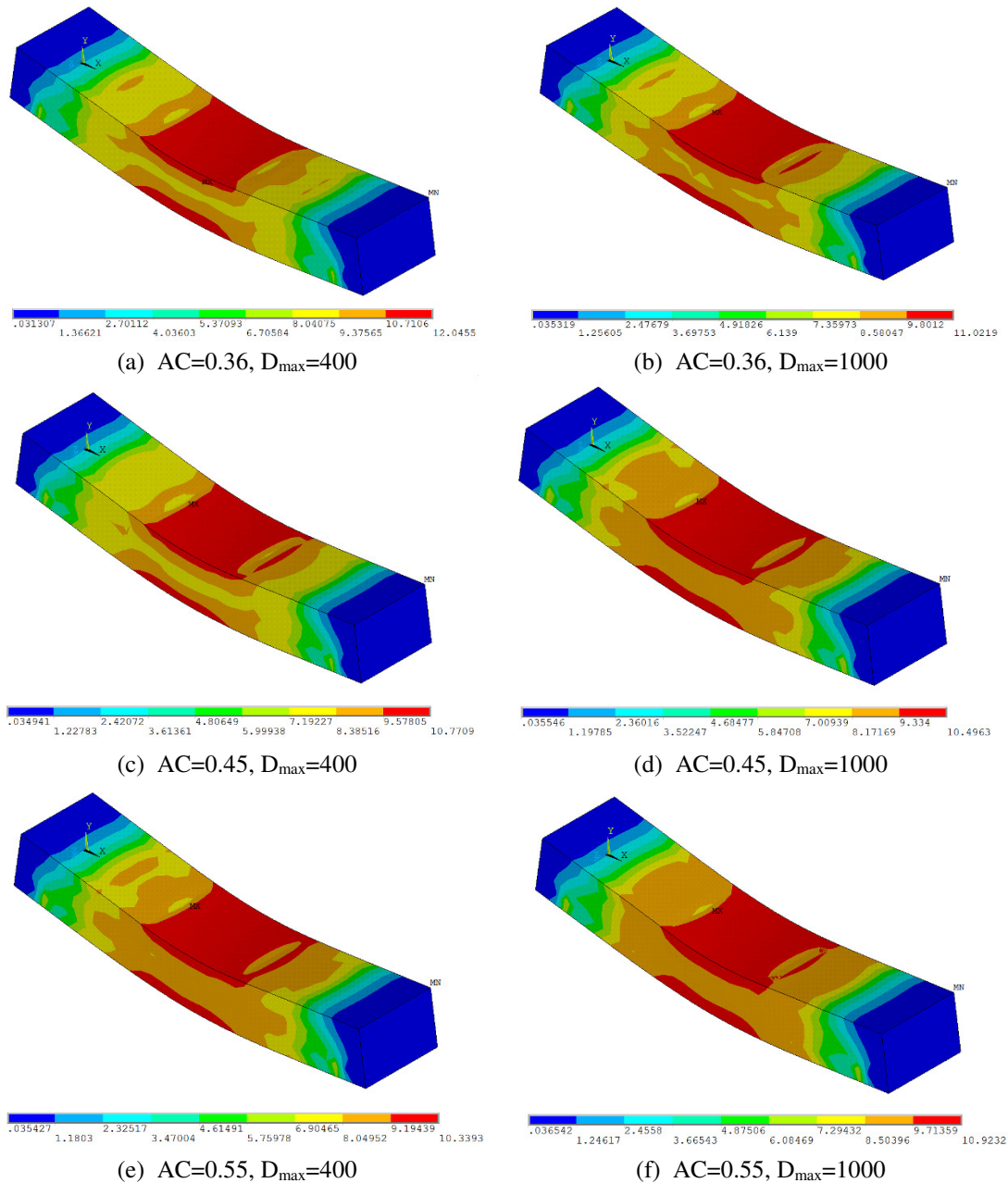


**Figure 5:** Contour plots of tensile stress for ECC beams

#### 4.4 Mid-Span Beam Deflection

Table 3 illustrates the flexural deflection property of ECC beams, which signifies the material ductility. It has been provided that the type and amount of mineral admixture, significantly depends upon total deflection of the ECC beam. In comparison to the MSC beam, that of FA-ECC exhibited better deflection abilities. This enhancement of deflection property in FA-ECC beams can be justified by the fact that utilizing FA is able to weaken the PVA fibre/matrix interface chemical linkage and reduce matrix (ECC without fibre) strength while strengthening the interface frictional bond [59]. Table 3 also demonstrates the correspondence between the statistical and experimental results providing that the average deflection from the numerical values for beams of aggregate size ranging from 400 and 1000  $\mu\text{m}$ , are larger than those obtained from the experimental results having a variance of 4.8%.

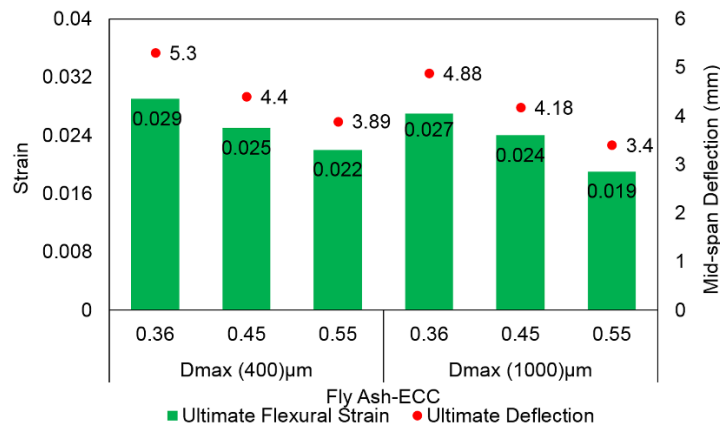


**Figure 6:** Influence of aggregate size and content on the flexural strain and deflection

In Table 3, the unwanted influence of enhanced size of aggregates on ductility performances can be easily observed. It is evident from the provided information that increases in aggregate size and quantity affects the ECC ductility and it decreases. The negative aspects of increasing aggregate may possibly be linked to the related poor dissipation of fibres. Required coating of fibres by the matrix is avoided by the balling of fibres supported by coarser aggregates at continuous aggregate content. Therefore, this affects a significant component that affects ductility i.e. effective fibre content [32]. In addition, a greater extent of aggregate interconnection is anticipated for ECCs with larger aggregate size and volume, giving out a greater matrix toughness, which results in the decrease in the margin to develop multiple cracking [27, 60].

It can be observed that when ECC beams are compared with MSC beam, development is demonstrated in terms of deflection. From experimental and numerical results, the average percentage deflection enhancement of 400 µm maximum aggregate size ECC beams whereas that of MSC beams were 1451.2% and 1315.6%, respectively. It is to be noted that the average enhancement percentage in deflection based on numerical and experiential outcomes for 1000 µm maximum aggregate size ECC beams were 1198% and 1314.3% respectively.

Other than ECC properties, characteristics and kinds of mineral admixture plus amount of the PVA fibres also determine the flexural behaviour of the beam specimens. Nonetheless, appropriate and suitable estimates of experimental outcomes can be provided by the simulation outcomes. It is to be noted that the techniques that are used to examine the flexural behaviour of the ECC are tested before they are implemented. The suggested numerical mechanism will be utilized to evaluate the impacts of various parameters on the mechanical behaviour of the ECC beams.

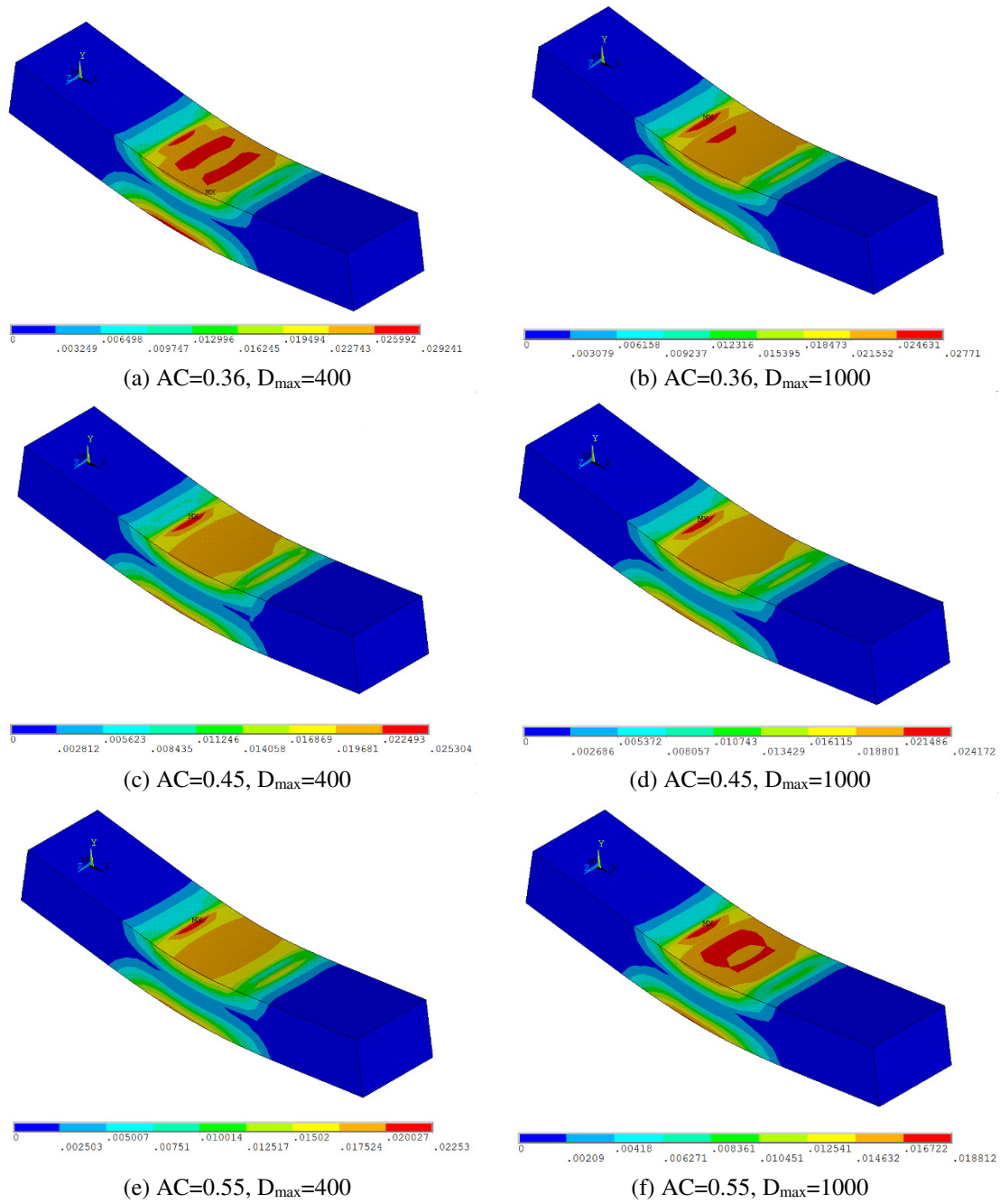


**Figure 7:** Contour plots of tensile strain for ECC beams

## 5.0 NONLINEAR PARAMETRIC STUDY

A nonlinear parametric study is carried out to evaluate the influence of parameters on the prediction of the flexural stress and flexural deflection of ECC beams in a 3D FE simulation, which comprises ECC aggregate content ( $AC$ ), and ECC compressive strength ( $f_{ECC}$ ) based on maximum aggregate size ( $D_{max}$ ). These parameters have been obtained using an exponential regression line. The exponential regression analysis resulted in higher  $R^2$  values (0.997) than other types of regression. This type of regression was used because it yielded a more realistic prediction of the flexural behaviour of ECC beams. To examine the reliability and validity of

the proposed new model, an extensive verification is carried out using a series of experimental data available in the literature [42, 43].

### 5.1 Influence of ECC Aggregate Content

The aggregate content is an important factor in the stiffness of the ECC beams. Fig. 8 illustrate the influence of the aggregate content on the likelihood of flexural stress, where, an increase in the aggregate content decreases the flexural stress of (400 and 1000)  $\mu\text{m}$  maximum aggregate size ECC beams by  $15.5e^{-0.526AC}$  and  $10.659e^{0.24AC}$ , respectively. Furthermore, the flexural deflection of (400 and 1000) maximum aggregate size ECC beams decreases with an increase in aggregate content by  $9.552e^{-1.664AC}$  and  $9.654e^{-1.884AC}$ , respectively, as shown in Fig. 9.

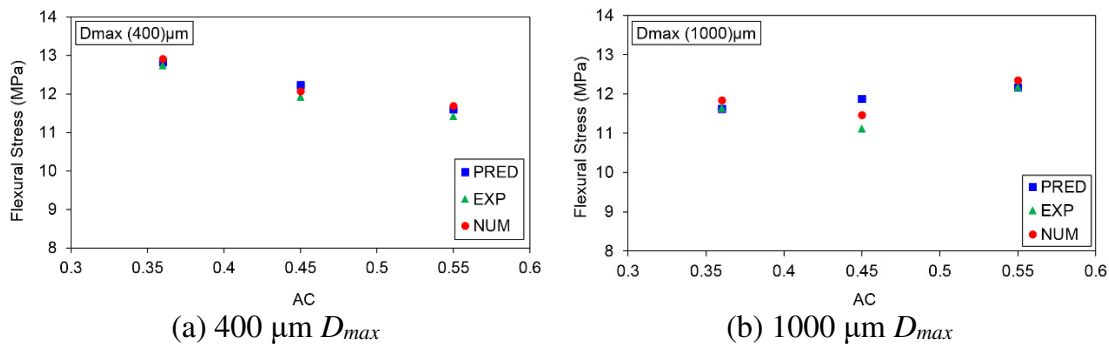


**Fig.8:** Influence of aggregate content on the flexural stress by comparing experimental, numerical, and predicted results of ECC beams

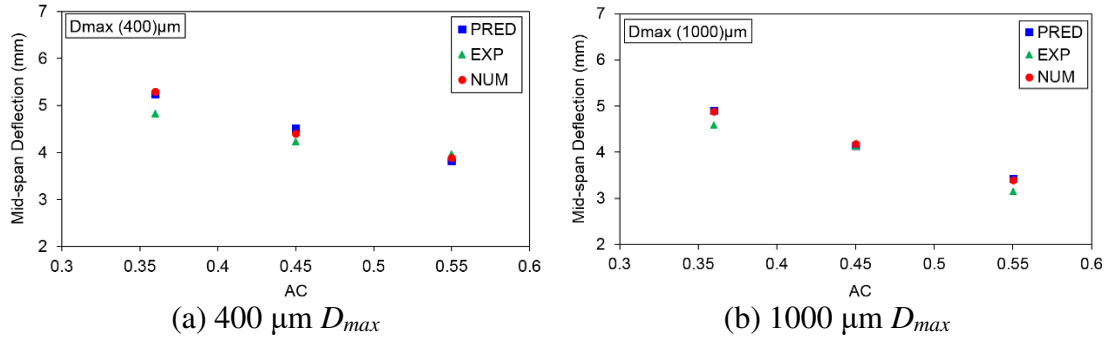


**Figure 9:** Influence of aggregate content on the deformability in flexure by comparing experimental, numerical, and predicted results of ECC beams

### 5.2 Influence of ECC Compressive Strength

The compressive strength is also an important factor in the stiffness of the ECC beams. Fig. 10 clarify the influence of the compressive strength on the likelihood of flexural stress, where, an increase in the compressive strength increases the flexural stress of (400 and 1000)  $\mu\text{m}$  maximum aggregate size ECC beams by  $6.714e^{0.009f_{ECC}}$  and  $7.916e^{0.006f_{ECC}}$ , respectively. Furthermore, the flexural deflection of 400  $\mu\text{m}$  maximum aggregate size ECC beams increases with an increase in compressive strength by  $0.619e^{0.03f_{ECC}}$  and decreases with an increase in compressive strength by  $61.523e^{-0.042f_{ECC}}$  for 1000  $\mu\text{m}$  maximum aggregate size ECC beams, as shown in Fig. 11.

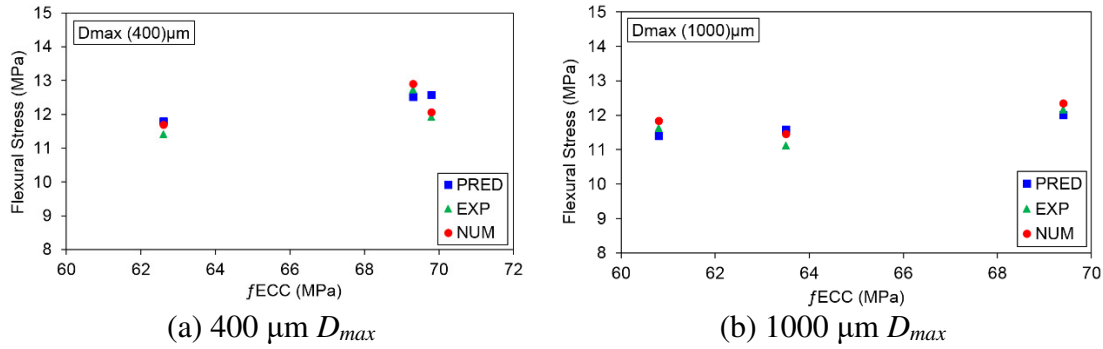


**Figure 10:** Influence of ECC compressive strength on the flexural stress by comparing experimental, numerical, and predicted results of ECC beams

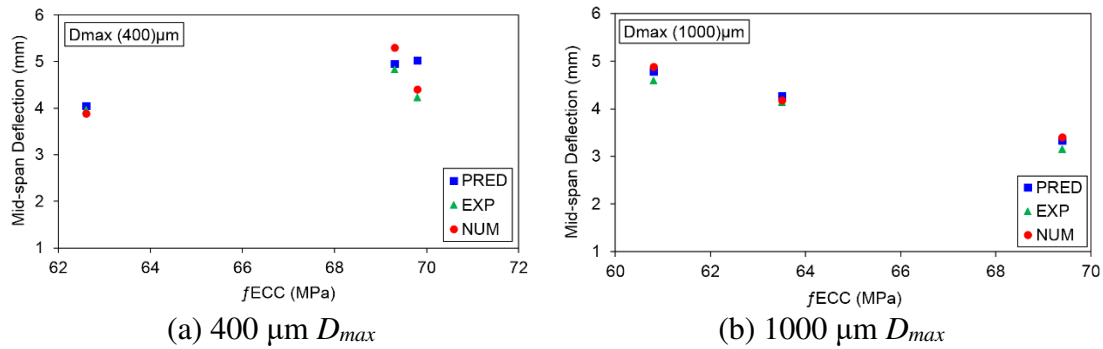


**Figure 11:** Influence of ECC compressive strength on the deformability in flexure by comparing experimental, numerical, and predicted results of ECC beams

### 5.3 Prediction of New Models

It is a well agreed notion that an ideal design of the ECC mixture having its factors in accordance with the micromechanical design theory necessarily requires to be an effective tool able to enhance the mechanical characteristics of hardened mixtures. However, there still exists the need to obtain comprehensive and precise information explaining the mechanical nature of ECC beams as per the provided conditions. Hence, to analyse the ultimate flexural stress ( $FS$ ) and ultimate flexural deflection ( $Def$ ) statistically, new models of correspondence have been designed on the basis of three major factors of ECC i.e. aggregate content ( $AC$ ), ECC compressive strength ( $f_{ECC}$ ), and maximum aggregate size ( $D_{max}$ ). Eqs. (7) and (8) illustrate these relations:

$$FS = \frac{0.893AC^{-0.148} D_{max}^{0.033}}{f_{ECC}^{-0.592}} \quad (7)$$

$$Def = \frac{8.183AC^{-0.688} D_{max}^{-0.14}}{f_{ECC}^{0.33}} \quad (8)$$

The experimental data provided in the literature was used to test the validity and constancy of the newly presented model. The considered data comprised of the results obtained from testing 57 ECC beams. It is observed that the data collected previously with regard to the geometric and mechanical properties were quite similar to that of data obtained through the said research. The results obtained from new model with respect to its validity are shown in Figs. 12 and 13 for maximum flexural stress and deflection. It can be seen that for  $FS_{Exp}/FS_{Pred}$  and  $Def_{Exp}/Def_{Pred}$

- the standard deviation values are 0.08, 0.13, respectively
- the mean values are 1.01 and 1.05, respectively
- the corresponding coefficients of variation ( $COV_s$ ) are 7.92%, 12.38%, respectively
- the coefficients of correlation,  $R$ , are 0.97, 0.95, respectively

This statistically proves the newly presented model as dependable for all of the ECC beams configurations employed in the experiment. Furthermore, these values include two lines indicating the presence of a  $\pm 10\%$  and  $\pm 13\%$  band regarding the provisions of the new model along with the experimental values for flexural stress and deflection results, respectively. These results lie within the range of these limitations while the new values are in agreement to the values obtained through experimental results.

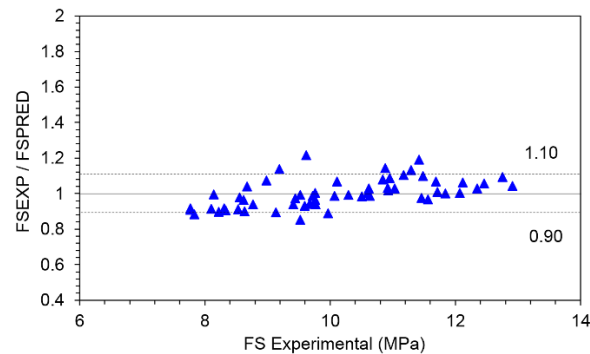


**Figure 12:** Predicted flexural stress by the new model in comparison with the experimental values

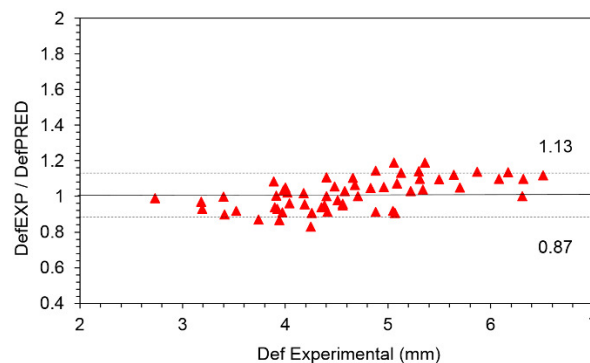


**Figure 13:** Predicted deflection by the new model in comparison with the experimental values

## 6.0 CONCLUSIONS

This research aims to analyse the potential effect of aggregate size and amount upon the mechanical performances of ECC beams by means of using nonlinear finite element model. To test the validity of models of the ECC beams operating under monotonic loading, experimental results were obtained. The results acquired from statistical evaluation were used to conduct the nonlinear parametric study to investigate the various parameters influencing the flexural stress and flexural deflection of ECC beams. Furthermore, new models of ECC were proposed which addressed the phenomenon on the basis of aggregate content ( $AC$ ), ECC compressive strength ( $f_{ECC}$ ), and maximum aggregate size ( $D_{max}$ ). A comparative analysis of the results obtained from the proposed models and that obtained from experimental analysis of 57 ECC beam as provided in the literature. These results can be summed up as:

- The model results showed that an increase in the aggregate size and quantity has no influence on the flexural strength, for the provided range of aggregate size. However, this change tends to reduce the ductility of ECC.
- When the ECC and MSC beams were subjected to comparative analysis, the ECC beams were observed to show an increase in flexural stress, strain, and mid-span deflection, having an average improvement percentage of 70.33%, 1116.67% and 1256.78%, respectively.
- As per the finite element analysis, the flexural stress- deflection property of the beams was in agreement with the results obtained from experiments. Nonetheless, the numerical values for average ultimate strength and deflection obtained for the beams are 2% and 4.8% larger than those obtained from the experimental results, respectively. In addition to the ECC properties, the flexural behaviour of the beam can also be identified through properties and nature of mineral admixture, and quantity of the PVA fibres. The accuracy of experimental results can only be obtained through replication of results. Furthermore, the numerical method to identify the flexural behaviour of the ECC beams is validated through these results.
- The nonlinear parametric study demonstrated that the mid-span beam deflection properties, through which material ductility, and flexural stress of ECC beams is indicated, are subjected to considerable variations with respect to changes in  $AC$  and  $f_{ECC}$  parameters. The deflection ability and flexural stress of the beams are in a negative relation with both of these factors.
- As per the comparative analysis with the experimental results, the newly proposed model is observed to be more precise to identify the flexural behaviour of the ECC beams. For  $FS_{Exp}/FS_{Pred}$  and  $Def_{Exp}/Def_{Pred}$ ;
  - The mean values are 1.01 and 1.05, respectively.
  - The corresponding coefficients of variation are 7.92%, 12.38%, respectively
  - The coefficients of correlation are 0.97, 0.95, respectively.
  - The error percentage to identify the flexural behaviour was less than 10% and 13%, respectively.

## ACKNOWLEDGEMENT

The researchers gratefully acknowledge the technical support provided by Faculty of Civil Engineering at University of Gaziantep.

## REFERENCES

- [1] Kunieda, M. and K. Rokugo, Recent Progress on HPFRCC in Japan Required Performance and Applications. Journal of Advanced Concrete Technology, 2006. 4(1): p. 19-33.
- [2] Lim, Y.M. and V.C. Li, Durable repair of aged infrastructures using trapping mechanism of engineered cementitious composites. Cement and Concrete Composites, 1997. 19(4): p. 373-385.
- [3] Fraternali, F., et al., Experimental study of the thermo-mechanical properties of recycled PET fiber-reinforced concrete. Composite Structures, 2011. 93(9): p. 2368-2374.

- [4] D'Ambrisi, A., L. Feo, and F. Focacci, Bond-slip relations for PBO-FRCM materials externally bonded to concrete. *Composites Part B-Engineering*, 2012. 43(8): p. 2938-2949.
- [5] D'Ambrisi, A., L. Feo, and F. Focacci, Experimental analysis on bond between PBO-FRCM strengthening materials and concrete. *Composites Part B-Engineering*, 2013. 44(1): p. 524-532.
- [6] Cho, C.G., et al., Cyclic responses of reinforced concrete composite columns strengthened in the plastic hinge region by HPFRC mortar. *Composite Structures*, 2012. 94(7): p. 2246-2253.
- [7] Balaguru, P.N. and S.P. Shah, *Fiber-reinforced cement composites*. 1992.
- [8] Hassan, N.Z., A.G. Sherif, and A.H. Zamarawy, Finite element analysis of reinforced concrete beams with opening strengthened using FRP. *Ain Shams Engineering Journal*, 2015.
- [9] Mahmoud, A.M., Finite element modeling of steel concrete beam considering double composite action. *Ain Shams Engineering Journal*, 2015.
- [10] Mahmoud, A.M., Finite element implementation of punching shear behaviors in shear-reinforced flat slabs. *Ain Shams Engineering Journal*, 2015.
- [11] Morsy, A. and E.T. Mahmoud, Bonding techniques for flexural strengthening of RC beams using CFRP laminates. *Ain Shams Engineering Journal*, 2013. 4(3): p. 369-374.
- [12] Mahmoud, A.M., Strengthening of concrete beams having shear zone openings using orthotropic CFRP modeling. *Ain Shams Engineering Journal*, 2012. 3(3): p. 177-190.
- [13] Li, V.C., Engineered Cementitious Composites - Tailored Composites Through Micromechanical Modeling. *Fiber Reinforced Concrete: Present and the Future* edited by N. Banthia, in *Fiber Reinforced Concrete: Present and the Future* edited by N. Banthia, A. Bentur, A. and A. Mufti, Canadian Society for Civil Engineering, Montreal, 1998: p. 64-97.
- [14] Li, V.C., S. Wang, and C. Wu, Tensile strain-hardening behavior of polyvinyl alcohol engineered cementitious composite (PVA-ECC). *ACI materials Journal*, 2001. 98(6).
- [15] Li, V.C., *Engineered Cementitious Composites (ECC) Material, Structural, and Durability Performance*. 2008.
- [16] Sahmaran, M. and V.C. Li, Influence of microcracking on water absorption and sorptivity of ECC. *Materials and Structures*, 2009. 42(5): p. 593-603.
- [17] Composites. *ACI Materials Journal*, 2008. 105(4): p. 358-366.
- [18] Zhang, J. and V.C. Li, Monotonic and fatigue performance in bending of fiber-reinforced engineered cementitious composite in overlay system. *Cement and Concrete Research*, 2002. 32(3): p. 415-423.
- [19] Li, V., Advances in ECC research. *Material science to application – a tribute to Surendra P. Shah*. ACI Bookstore, 2002: p. 73–400.
- [20] Lin, Z. and V.C. Li, Crack bridging in fiber reinforced cementitious composites with slip-hardening interfaces. *Journal of the Mechanics and Physics of Solids*, 1997. 45(5): p. 763-787.

- [21] Hawileh, R.A., Finite element modeling of reinforced concrete beams with a hybrid combination of steel and aramid reinforcement. *Materials & Design*, 2015. 65: p. 831-839.
- [22] Zhang, J., C.K.Y. Leung, and Y.N. Cheung, Flexural performance of layered ECC-concrete composite beam. *Composites Science and Technology*, 2006. 66(11-12): p. 1501-1512.
- [23] Maalej, M. and V.C. Li, Introduction of strain-hardening engineered cementitious composites in design of reinforced concrete flexural members for improved durability. *ACI Structural Journal*, 1995. 92(2).
- [24] Li, V.C., From Micromechanics To Structural Engineering -- The Design Of Cementitious Composites For Civil Engineering Applications. *JSCE J. of Struc. Mechanics and Earthquake Engineering*, 1993. 10(2): p. 37-48.
- [25] Lin, Z., T. Kanda, and V.C. Li, On interface property characterization and performance of fiber reinforced cementitious composites. *Concrete Science and Engineering*, 1999. 1(3): p. 173-184.
- [26] Maruta, M., et al., New high-rise RC structure using pre-cast ECC coupling beam. *Concrete Journal*, 2005. 43(11): p. 18-26.
- [27] Li, V.C., D.K. Mishra, and H.-C. Wu, Matrix design for pseudo-strain-hardening fibre reinforced cementitious composites. *Materials and Structures*, 1995. 28(10): p. 586-595.
- [28] Dhawale, A. and V. Joshi, Engineered cementitious composites for structural applications. *International journal of application or Innovation in Engineering & Management*, 2013. 2: p. 198-205.
- [29] Nallathambi, P., B. Karihaloo, and B. Heaton, Effect of specimen and crack sizes, water/cement ratio and coarse aggregate texture upon fracture toughness of concrete. *Magazine of Concrete Research*, 1984. 36(129): p. 227-236.
- [30] Perdikaris, P.C. and A. Romeo, Size effect on fracture energy of concrete and stability issues in three-point bending fracture toughness testing. *ACI Materials Journal*, 1995. 92(5).
- [31] De Koker, D. and G. Van Zijl. Extrusion of engineered cement-based composite material. in *Proceedings of the 6th RILEM Symposium on Fiber-Reinforced Concretes (FRC)*. 2004. Citeseer.
- [32] Parviz soroushian, M.N. and A.M. Jer-Wen Hsu, Optimization of the use of lightweight aggregates in carbon fiber reinforced cement. *ACI Materials Journal*, 1992. 89(3).
- [33] Fischer, G. and V.C. Li, Deformation behavior of fiber-reinforced polymer reinforced engineered cementitious composite (ECC) flexural, members under reversed cyclic loading conditions. *Aci Structural Journal*, 2003. 100(1): p. 25-35.
- [34] Kim, J.-K., et al., Tensile and fiber dispersion performance of ECC (engineered cementitious composites) produced with ground granulated blast furnace slag. *Cement and Concrete Research*, 2007. 37(7): p. 1096-1105.
- [35] Zhou, J., et al., Development of engineered cementitious composites with limestone powder and blast furnace slag. *Materials and Structures*, 2010. 43(6): p. 803-814.
- [36] Wang, S.X. and V.C. Li, Engineered cementitious composites with high-volume fly ash. *Aci Materials Journal*, 2007. 104(3): p. 233-241.

- [37] Yang, D.S., S.K. Park, and K.W. Neale, Flexural behaviour of reinforced concrete beams strengthened with prestressed carbon composites. *Composite Structures*, 2009. 88(4): p. 497-508.
- [38] Nematollahi, B., J. Sanjayan, and F.U. Ahmed Shaikh, Tensile Strain Hardening Behavior of PVA Fiber-Reinforced Engineered Geopolymer Composite. *Journal of Materials in Civil Engineering*, 2015: p. 04015001.
- [39] Said, S.H., H.A. Razak, and I. Othman, Flexural behavior of engineered cementitious composite (ECC) slabs with polyvinyl alcohol fibers. *Construction and Building Materials*, 2015. 75: p. 176-188.
- [40] Pan, Z.F., et al., Study on mechanical properties of cost-effective polyvinyl alcohol engineered cementitious composites (PVA-ECC). *Construction and Building Materials*, 2015. 78: p. 397-404.
- [41] Said, S.H. and H.A. Razak, The effect of synthetic polyethylene fiber on the strain hardening behavior of engineered cementitious composite (ECC). *Materials & Design*, 2015. 86: p. 447-457.
- [42] Şahmaran, M., et al., Influence of aggregate type and size on ductility and mechanical properties of engineered cementitious composites. *ACI Materials Journal*, 2009. 106(3): p. 308-316.
- [43] Şahmaran, M., et al., Improving the workability and rheological properties of Engineered Cementitious Composites using factorial experimental design. *Composites Part B: Engineering*, 2013. 45(1): p. 356-368.
- [44] Sahmaran, M., et al., Combined Effect of Aggregate and Mineral Admixtures on Tensile Ductility of Engineered Cementitious Composites. *Aci Materials Journal*, 2012. 109(6): p. 627-637.
- [45] Manual, A.U.s., Version (15). Swanson Analysis Systems Inc, 2014.
- [46] Willam, K. and E. Warnke. Constitutive model for the triaxial behavior of concrete. in *Proceedings, international association for bridge and structural engineering*. 1975. ISMES, Bergamo, Italy.
- [47] Kwan, A., H. Dai, and Y. Cheung, Non-linear seismic response of reinforced concrete slit shear walls. *Journal of sound and vibration*, 1999. 226(4): p. 701-718.
- [48] Terec, L., T. Bugnariu, and M. Pastrav, Non-Linear Analysis of Reinforced Concrete Frames Strengthened with Infilled Walls. *Revista Romana De Materiale-Romanian Journal of Materials*, 2010. 40(3): p. 214-221.
- [49] Damian, K., et al., Finite element modeling of reinforced concrete structures strengthened with FRP laminates. Report for Oregon Department Of Transportation, Salem, 2001.
- [50] Raongjant, W. and M. Jing. Finite element analysis on lightweight reinforced concrete shear walls with different web reinforcement. in *The Sixth Prince of Songkla Univ. Engng. Conf., Hat Yai, Thailand*. 2008.
- [51] Wolanski, A.J., Flexural behavior of reinforced and prestressed concrete beams using finite element analysis. 2004, Citeseer.
- [52] Leung, C.K.Y. and Q.A. Cao, Development of pseudo-ductile permanent formwork for durable concrete structures. *Materials and Structures*, 2010. 43(7): p. 993-1007.

- [53] Zhou, J., J. Pan, and C. Leung, Mechanical Behavior of Fiber-Reinforced Engineered Cementitious Composites in Uniaxial Compression. *Journal of Materials in Civil Engineering*, 2014.
- [54] Kanda, T., Z. Lin, and V.C. Li, Tensile stress-strain modeling of pseudostrain hardening cementitious composites. *Journal of Materials in Civil Engineering*, 2000. 12(2): p. 147-156.
- [55] Yuan, F., J. Pan, and C. Leung, Flexural behaviors of ECC and concrete/ECC composite beams reinforced with basalt fiber-reinforced polymer. *Journal of Composites for Construction*, 2013.
- [56] Cetin, A. and R.L. Carrasquillo, High-performance concrete: influence of coarse aggregates on mechanical properties. *ACI Materials Journal*, 1998. 95(3).
- [57] Baalbaki, W., et al., Influence of coarse aggregate on elastic properties of high-performance concrete. *ACI Materials Journal*, 1991. 88(5).
- [58] Aïtcin, P.-C. and P.K. Mehta, Effect of coarse aggregate characteristics on mechanical properties of high-strength concrete. *ACI Materials Journal*, 1990. 87(2).
- [59] Li, V., From micromechanics to structural engineering – the design of cementitious composites for civil engineering applications. *Struct Eng Earthq Eng Jpn Soc Civ Eng*, 1993. 10(2): p. 37–48.
- [60] Li, V.C., Engineered Cementitious Composites (Ecc)–Tailored Composites Through Micromechanical Modeling *Micromechanical*, T.C.T., 1998.